Stepwise and Concerted Pathways in Photoinduced and Thermal Electron-Transfer/Bond-Breaking Reactions. Experimental Illustration of Similarities and Contrasts

Laurence Pause, Marc Robert, and Jean-Michel Savéant*

Contribution from the Laboratoire d'Electrochimie Moléculaire, Unité Mixte de Recherche Université-CNRS No 7591, Université de Paris 7-Denis Diderot, 2 place Jussieu, 75251 Paris Cedex 05, France

Received December 11, 2000. Revised Manuscript Received March 14, 2001

Abstract: The electrochemical (cyclic voltammetry) and photoinduced (fluorescence quenching, quantum yields) reductive cleavages of four compounds, 4-cyano-α-trifluorotoluene (**1**), dimethylphenyl sulfonium (**2**), 4-cyanobenzylmethylphenyl sulfonium (**3**), and 4-cyanobenzyl chloride (**4**), are investigated and compared in terms of concerted vs stepwise mechanisms. Bearing in mind that an increase of the thermodynamic driving force shifts the mechanism from concerted to stepwise and that the driving force is larger under photochemical than under electrochemical conditions, **1** and **2** are typical examples where a stepwise mechanism is followed with compatible kinetic characteristics under both regimes. **4** undergoes a concerted electrochemical reductive cleavage, and the same mechanism is followed in the photoinduced reaction with consistent kinetic characteristics. The case of **3** is of particular interest, since a trend of passing from a concerted to a stepwise mechanism when going from the electrochemical to the photochemical conditions indeed appears upon analysis of the experimental results. The change of mechanism is, however, not complete since, in the photoinduced reaction, there is a balanced competition between the two pathways. In the same families of compounds, the unsubstituted benzylmethylphenyl sulfonium cations shows such a borderline behavior during the electrochemical reaction. In the photoinduced reaction, it is the 4-cyano derivative which behaves in a borderline manner, in line with the fact that it gives rise more readily to a concerted mechanism than the unsubstituted compound.

Coupling of electron transfer with the cleavage of a chemical bond appears as a central problem in understanding the general reactivity laws of electron-transfer chemistry.[1] Such bond-cleaving electron transfers may be triggered photochemically or thermally (heterogeneously, i.e., electrochemically, or homogeneously).[2,3] An important issue in both cases is to know whether electron transfer and bond cleavage are concerted or successive (Scheme 1) and what factors control the occurrence of the two mechanisms and the passage from one to the other.

With electrochemical reactions, the transition between the two reaction pathways has been observed within families of cleaving substrates upon varying their molecular properties.[4] It has also been predicted[5a] and experimentally demonstrated[4c,5b−d] that the mechanism may pass from concerted to stepwise upon increasing the thermodynamic driving force offered to the reaction. The same two phenomena have been experimentally confirmed with homogeneous electron-transfer reactions, too.[6] However, in this case, the unambiguous demonstration of a passage from a concerted to a stepwise mechanism upon increasing the thermodynamic driving force required a kinetic amplification allowing the investigation of a domain of very low driving forces.[6b]

Scheme 1

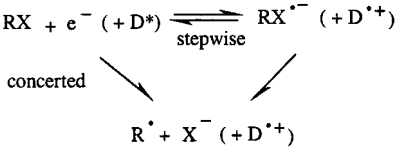

The case of photoinduced reactions was more problematic. It has long been believed on intuitive grounds that dissociative electron-transfer reactions (i.e., reactions following the concerted

(1) (a) It may also be an important issue in the present development of molecular electronics insofar as electron-transfer properties of molecules appear as good guidelines for designing molecular devices (see, e.g., ref 1b and references therein). (b) Wong, E. W.; Collier, C. P.; Bhloradsk, M.; Raymo, F. M.; Stoddart, J. F.; Heath, J. R. *J. Am. Chem. Soc.* **2000**, *122*, 5831.

(2) (a) Saeva, F. D. *Top. Curr. Chem.* **1990**, *156*, 61. (b) Saeva, F. D Intramolecular Photochemical Electron Transfer (PET)—Induced Bond Cleavage Reactions in some Sulfonium Salts Derivatives. In *Advances in Electron Transfer Chemistry*; Mariano, P. S., Ed.; JAI Press: New York, 1994; Vol. 4, pp 1−25. (c) Gaillard, E. R.; Whitten, D. G. *Acc. Chem. Res.* **1996**, *29*, 292.

(3) (a) Savéant, J.-M. Electron Transfer, Bond Breaking and Bond Formation. In *Advances in Physical Organic Chemistry*; Tidwell, T. T., Ed.; Academic Press: New York, 2000; Vol. 35, pp 117−192. (b) Hush, N. S. *J. Electroanal. Chem.* **1999**, *470*, 170. (c) Maletin, Y. A.; Cannon, R. D. *Theor. Exper. Chem.* **1998**, *34*, 7. (d) Lund, H.; Daasbjerg, K.; Lund, T.; Occhialini, D.; Pedersen, S. U. *Acta Chem Scand.* **1997**, *51*, 135. (e) Lund, H.; Daasbjerg, K.; Lund, T.; Pedersen, S. U. *Acc. Chem. Res.* **1995**, *28*, 313. (f) Savéant, J.-M. Dissociative Electron Transfer. In *Advances in Electron Transfer Chemistry*; Mariano, P. S., Ed.; JAI Press: New York, 1994; Vol. 4, pp 53−116. (g) Savéant, J.-M. *Acc. Chem. Res.* **1993**, *26*, 455. (h) Savéant, J.-M. Single Electron Transfer and Nucleophilic Substitution. In *Advances in Physical Organic Chemistry*; Bethel, D., Ed.; Academic Press: New York, 1990; Vol. 26, pp 1−130.

(4) (a) Andrieux, C. P.; Le Gorande, A.; Savéant, J.-M. *J. Am. Chem. Soc.* **1992**, *114*, 6892. (b) Andrieux, C. P.; Differding, E.; Robert, M.; Savéant, J.-M. *J. Am. Chem. Soc.* **1993**, *115*, 6592. (c) Andrieux, C. P.; Robert, M.; Saeva, F. D.; Savéant, J.-M. *J. Am. Chem. Soc.* **1994**, *116*, 7864. (d) Andrieux, C. P.; Tallec, A.; Tardivel, R.; Savéant, J.-M.; Tardy, C. *J. Am. Chem. Soc.* **1997**, *119*, 2420.

(5) (a) Andrieux, C. P.; Savéant, J.-M. *J. Electroanal. Chem.* **1986**, *205*, 43. (b) Antonello, S.; Maran, F. *J. Am. Chem. Soc.* **1997**, *119*, 12595. (c) Pause, L.; Robert, M.; Savéant, J.-M. *J. Am. Chem. Soc.* **1999**, *121*, 7158. (d) Antonello, S.; Maran, F. *J. Am. Chem. Soc.* **1999**, *121*, 9668.

(6) (a) Severin, M. G.; Farnia, E.; Vianello, E.; Arévalo, M. C. *J. Electroanal. Chem.* **1988**, *251*, 369. (b) Costentin, C.; Hapiot, P.; Médebielle, M. Savéant, J.-M. *J. Am. Chem. Soc.* **1999**, *121*, 4451.

10.1021/ja004234u CCC: $20.00
Published on Web 05/08/2001

Table 1. Mechanisms and Quantum Yields

Mechanism	Quantum yield
Concerted 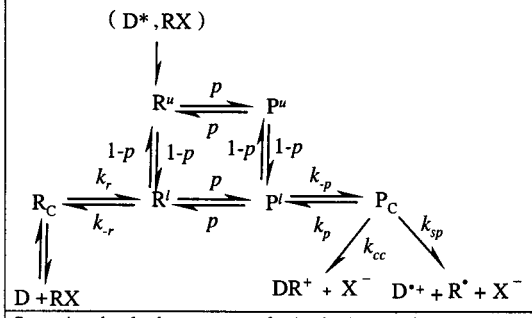	$\Phi = \dfrac{1}{(1+p)\left(1+\dfrac{2p}{1+p}\dfrac{k_{-act}}{k_{sp}+k_{cc}}\right)}$ (1)
Stepwise, back electron transfer in the inverted region 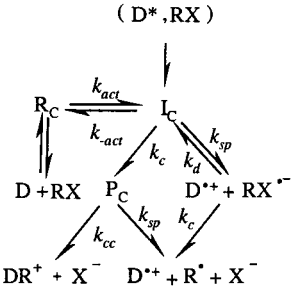	$\Phi = \dfrac{k_{sp}+k_c}{k_{sp}+k_c+k_{-act}}$ (2)
Stepwise, back electron transfer in the normal region 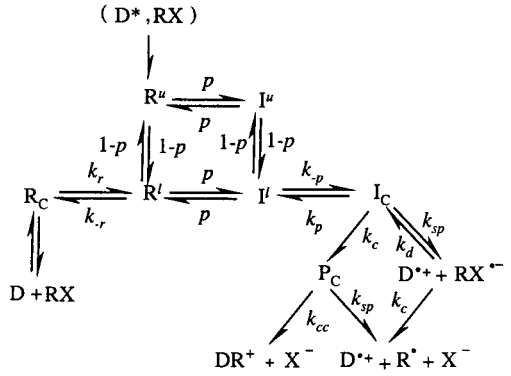	$\Phi = \dfrac{1}{(1+p)\left(1+\dfrac{2p}{1+p}\dfrac{k_{-act}}{k_{sp}+k_c}\right)}$ (3)
R_C:(D,RX) I_C:($D^{\bullet+}$, $RX^{\bullet-}$) P_C:($D^{\bullet+}$, $R^{\bullet}$, X^-) R^l, I^l, P^l, R^u, I^u, P^u are reactant, intermediate and product states on the lower and upper potential energy surfaces near their intersection, respectively. [8a,b]	$p = 1-\exp\left\{-\dfrac{\pi^{3/2}H^2}{h\nu(RT)^{1/2}(D+\lambda_0)^{1/2}}\right\}$ (4) p is the probability that the system remains on the first-order potential energy surfaces formed by combination of the zero-order potential surfaces near their intersection. For the definition of ν, H, D and λ_0, see text.

mechanism) are necessarily endowed with a quantum yield for complete quenching equal to unity.[2c,7] Since, in all investigated cases, the quantum yield was definitely smaller than 1, it was inferred that the reaction mechanism was of the stepwise type, in contrast, in most circumstances, to the conclusions reached upon examination of thermal electron transfer to the same substrate. Particularly remarkable in this connection is the reduction of the 4-cyanobenzylmethylphenyl sulfonium cation because great care was taken, in the photoinduced reaction, to avoid, by an appropriate choice of the donors, the occurrence of electron transfer between the donor cation radical and the 4-cyanobenzyl radical, followed by regeneration of the starting sulfonium cation by coupling of the resulting 4-cyanobenzyl cation with methylphenyl sulfide, thus wasting a part of the photochemical energy. Avoiding this type of side reaction is indeed crucial in studies aiming at relating the quantum yield with the dissociative character of the electron-transfer/bond-breaking process.

Since then, however, it has been shown on theoretical grounds that photoinduced dissociative electron transfers are not necessarily endowed with quantum yields equal to unity.[8a] As recalled in Table 1, they are in fact related to the probability, p, that the system remains on the first-order potential energy surfaces formed by combination of the zero-order potential surfaces near

(7) (a) Arnold, B. R.; Scaiano, J. C.; McGimpsey, W. G. *J. Am. Chem. Soc.* **1992**, *114*, 9978. (b) Chen, L.; Farahat, M. S.; Gaillard, E. R.; Gan, H.; Farid, S.; Whitten, D. G. *J. Am. Chem. Soc.* **1995**, *117*, 6398. (c) Chen, L.; Farahat, M. S.; Gaillard, E. R.; Farid, S.; Whitten, D. G. *J. Photochem. Photobiol. A: Chem.* **1996**, *95*, 21. (d) Wang, X.; Saeva, F. D.; Kampmeier, J. A. *J. Am. Chem. Soc.* **1999**, *121*, 4364.

(8) (a) Robert, M.; Savéant, J.-M. *J. Am. Chem. Soc.* **2000**, *122*, 514. (b) Costentin, C.; Robert, M.; Savéant, J.-M. *J. Phys. Chem. A.* **2000**, *104*, 7492.

Scheme 2

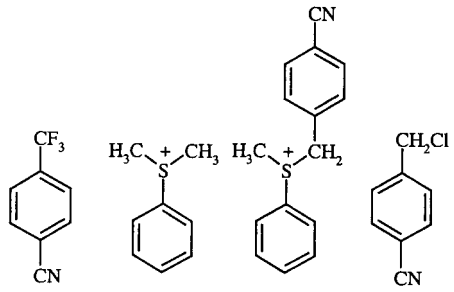

their intersection (eq 1).[8a] p is itself a function of the electronic coupling matrix element, H, and also of ν, the effective frequency at which the system crosses the intersection region, D, the dissociation energy of the cleaving bond, and λ_0, the solvent reorganization energy (eq 4). The quantum yield additionally depends on the competition between back electron transfer within the caged fragment cluster (rate constant, k_{-act}) on one hand and separation of fragments (rate constant, k_{sp}) and cage coupling of $R^{\bullet}$ and $D^{\bullet+}$ (rate constant, k_{cc}) on the other. Even in the case where the competition is strongly in disfavor of back electron transfer, the quantum yield, then simply given by $1/(1 + p)$, has no reason to be unity since this would imply that $H = 0$, i.e., that the ground-state electron transfer is totally nonadiabatic, a very unlikely circumstance.

With stepwise mechanisms, the expression of the quantum yield depends on whether the initial electron transfer occurs in the inverted or in the normal region.[8b] In the first case, it is given by eq 2 according to the mechanism depicted in Table 1. It is a function of the competition between back electron transfer from the caged fragment cluster (rate constant, k_{-act}) on one hand and separation of fragments (rate constant, k_{sp}) and cleavage of the intermediate anion radical on the other (rate constant, k_c). It is interesting to note that there is no reason that the quantum yield may not reach 1 (it suffices that the competition is strongly in disfavor of back electron transfer as compared to escape from the cage and cleavage of the intermediate), as opposed to the case of a dissociative electron transfer, a rather counterintuitive conclusion.

When back electron transfer occurs in the normal region, we again find an electronic coupling matrix element limitation, as appears in the expression of the quantum yield in eq 3, corresponding to the reaction scheme depicted in Table 1.[8b] Equation 4 still applies, making $D = (D_{RX}^{1/2} - D_{RX^{\bullet-}}^{1/2})^2$ (the D's are the homolytic bond dissociation energies of the subscript species). In this case, too, as for dissociative electron transfer, it is unlikely that the quantum yield may reach unity, even if the competition between back electron transfer from the caged fragment cluster on one hand and separation of fragments and cleavage of the intermediate anion radical on the other is strongly in disfavor of the former reaction.

The aim of the work reported below was to illustrate experimentally these various theoretical predictions, most of which do not match common intuition. For this purpose we selected the four substrates depicted in Scheme 2.[9] **1** and **2** are examples of compounds undergoing a stepwise reductive cleavage, with a slow and fast decomposing anion radical, respectively. Compound **4** follows a concerted mechanism when the electron transfer is performed electrochemically. The question then arises of whether the measured quantum yields are consistent with the same mechanism or with a stepwise mechanism. The last issue that will be discussed is as follows. Do the quantum yields measured for the photoinduced reduction of **3**[7d] indicate a concerted mechanism as observed in electrochemistry,[4d] or a stepwise mechanism that would result from the larger driving force offered by the photochemical induction as compared to the electrochemical reduction? Since **2** and **3** are positively charged molecules, the symbolism in Scheme 1 and in the rest of the paper implies, for these cases, that X bears one positive charge in RX, and thus that the leaving group X^- is in fact a neutral species.

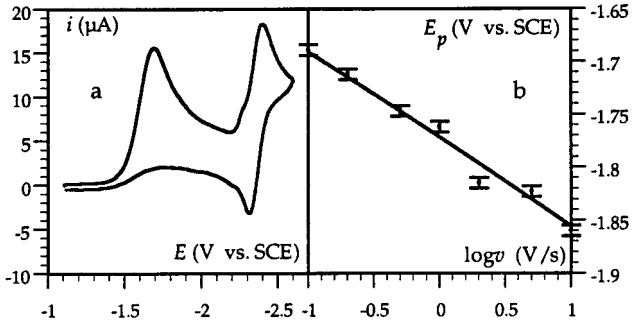

Figure 1. Cyclic voltammetry of **4** (1.14 mM) in DMF + n-Bu_4NBF_4 at 293 K on a glassy carbon disk electrode. (a) Cyclic voltammogram at 0.1 V/s. (b) Variation of the peak potential with the scan rate. Full line: theoretical variation (see the Discussion section).

Results

Electrochemical Reactions. Detailed reports on the electrochemistry of **1** and **3** are available in the literature and will be used in the subsequent discussion.[4c,10] Figure 1 shows a typical cyclic voltammogram obtained with **4**. A first irreversible wave is observed around −1.70 V vs SCE at low scan rate, while a one-electron reversible wave is obtained at more negative potentials (standard potential, −2.37 V vs SCE). The second wave is identical to the reduction wave of 4-cyanotoluene, the product expected for a $2e^- + H^+$ reductive cleavage at the first cathodic process. The electron stoichiometry at the first wave varies from 1.5 to 1.9 between 0.1 and 10 V/s. These observations, already made with the bromo derivative,[4a] are similarly indicative of the following set of events. The reductive cleavage, taking place at the first wave, produces the 4-cyanobenzyl radical, which is easier to reduce than the starting compound. The corresponding carbanion thus formed may react with the starting compound according to an S_N2 reaction, in competition with its protonation by residual water. An approximately 10-fold excess of acetic acid was added to the solution in order to avoid the possible influence of the S_N2 reaction on the peak characteristics. The shape of the voltammograms remains almost unchanged, and the peak potential shifts positively by ca. 30 mV. The peak potential varies in an approximately linear manner with the logarithm of the scan rate by −81 mV per unit between 0.1 and 10 V/s (Figure 1), thus leading to an average value of 0.36_5 for the transfer coefficient α.[11] These data, as well as the large separation between the

(9) (a) So far, the only case that has been examined in detail is the thermal[9b] and photoinduced[9c] dissociative electron transfers to carbon tetrachloride. (b) Pause, L.; Robert, M.; Savéant, J.-M. *J. Am. Chem. Soc.* **2000**, *112*, 9829. (c) Pause, L.; Robert, M.; Savéant, J.-M. *ChemPhysChem* **2000**, *1*, 199.

(10) Andrieux, C. P.; Combellas, C.; Kanoufi, F.; Savéant, J.-M.; Thiébault, A. *J. Am. Chem. Soc.* **1997**, *119*, 9527.

(11) (a) Nadjo, L.; Savéant, J.-M. *J. Electroanal. Chem.* **1973**, *48*, 113. (b) Andrieux, C. P.; Savéant, J.-M. In *Electrochemical Reactions in Investigation of Rates and Mechanisms of Reactions, Techniques of Chemistry*; Bernasconi, C. F., Ed.; Wiley: New York, 1986; Vol. VI/4E, Part 2, pp 305−390.

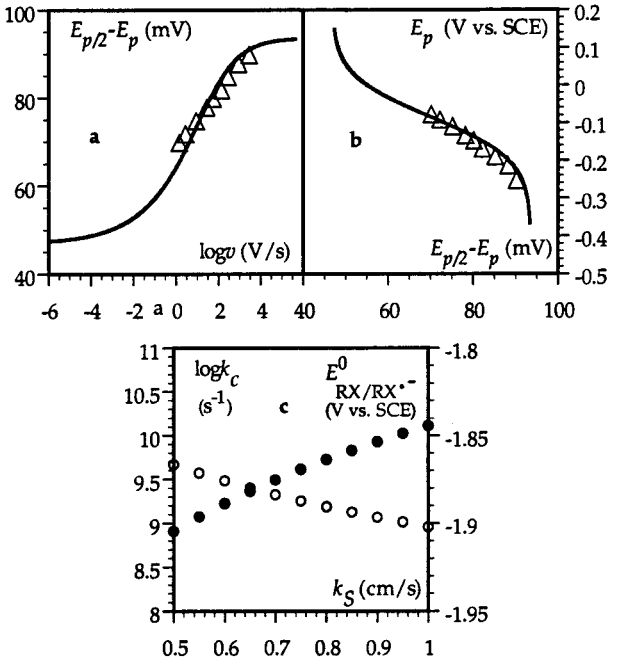

Figure 2. Cyclic voltammetry of **2** (2 mM) in DMF + *n*-Bu_4NBF_4 at 298 K on a glassy carbon disk electrode. (a) Variation of the peak width with the scan rate. (b) Variation of the peak potential with the peak width. The solid lines in (a) and (b) represent the best fitting of the experimental data with the theoretical curves (see text). (c) Variations of the cleavage rate constant (○) and standard potential (●) with the value selected for the standard rate constant of electron transfer.

first and second peak potentials (ca. 700 mV), point to a mechanism in which the cleavage of the C−Cl bond is concerted with the electron transfer.[3] The quantitative characteristics of the reaction will be examined in the Discussion section.

The reductive cleavage of **2** has been shown to follow a stepwise mechanism.[4c] For the purpose of the ensuing discussion, it is interesting to estimate the magnitudes of the standard potential, E^0, for the electron uptake and the rate constant for the cleavage step, k_c. The values of the peak width (i.e., the difference between the half-peak and the peak potentials, $E_{p/2} - E_p$), displayed in Figure 2a, and the variations of the peak potential with the scan rate (Figure 2b) indicate that the kinetics of the reaction are controlled jointly by the electron transfer and the cleavage steps. The $E_{p/2} - E_p$ vs log v may be fitted with a theoretical curve by sliding along the horizontal axis, thus allowing the determination of the constant $(F/2RT)(k_cD_d^2/k_S^4) = 1.4$ s/V (assuming, as seems reasonable, that the transfer coefficient is close to 0.5).[12] The variations of E_p with $E_{p/2} - E_p$ may likewise be fitted with a theoretical curve by sliding along the vertical axis this time, allowing the determination of $E^0_{RX/RX^{\bullet-}} + (RT/F)\ln(k_cD_d/k_S^2) = -1.6$ V vs SCE.[12] k_c and E^0 may be derived from these two relationships, provided k_S is known. The variations of k_c and E^0 with k_S are displayed in Figure 2c for $0.5 \le k_S \le 1$ cm/s,[13] a reasonable range of values in view of the size of **2** (as compared, e.g., to $k_S = 3$ cm/s for the dimethylanthracenyl sulfonium cation[4c,13]).

Photoinduced Reactions. The data concerning **3** are available from ref 7d. We repeated and confirmed these data, gauging the amount of the 4-cyanobenzylmethyl sulfide formed by means of its anodic cyclic voltammetric wave instead of gas chromatography as used in ref 7d.

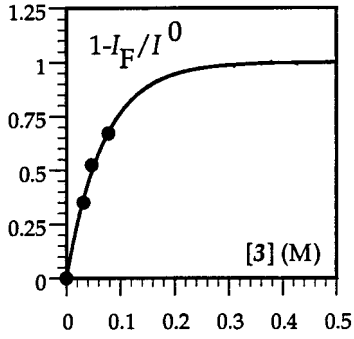

Figure 3. Fluorescence quenching of ^{1}EDA by **4**. I_F and I^0 represent fluorescence intensity in the presence and in the absence of quencher, respectively.

Table 2. Complete Quenching Quantum Yields and Rate Constants of Photoinduced Electron Transfer

cleaving acceptor	sensitizer	Φ^∞	k_{et} (M^{-1} s^{-1})
1	perylene	0.25 ± 0.04	(2−5) × 10^8
2	EDA	0.35 ± 0.05	(0.5−2.5) × 10^8
3	EDA	0.77 ± 0.02	(0.6−1.6) × 10^{10} [a]
4	EDA	0.55 ± 0.08	10^9

[a] From ref 7d.

In the case of **4**, we used 2-ethyl-9,10-dimethoxyanthracene (EDA) as sensitizer. Fluorescence quenching of ^{1}EDA by **4** is fast enough (Figure 3) for complete quenching to be reached for reasonable values of the concentration of quencher. It was thus possible to use the same strategy as for CCl_4[9c] for the determination of Φ^∞, namely continuous irradiation of the reaction mixture at a concentration of quencher corresponding to complete quenching. The quantum yield was derived, like with CCl_4,[9c] from the amount of Cl^- formed, as measured by ion chromatography. With concentrations of 1.8 and 1.85 M, the value of the complete quenching quantum yield reported in Table 2 was found. Laser flash irradiation combined with spectrophotometric monitoring of $EDA^{\bullet+}$, following the same procedure as that already used with CCl_4,[9c] allowed the determination of the quantum yield for the formation of $D^{\bullet+}$ (see Experimental Section). For example, at a concentration of **4** equal to 1.3 M, $\Phi_{D^{\bullet+}} = 0.16$, while Φ derived from the formation of Cl^- in a continuous irradiation experiment at the same concentration is equal to 0.4.

Fluorescence quenching of ^{1}EDA by **2** and **1** is slower (Figure 4). With **1**, we use in fact perylene as sensitizer, for it is slightly more efficient than EDA. Since complete quenching would be reached for unreasonably high quencher concentrations for **1** and **2**, Φ^∞ was determined by the extrapolation procedure depicted in Figure 4, thus leading to the values listed in Table 2. With **2**, the quantum yield was derived from the chromatographic determination of the amount of methylphenyl sulfide formed in continuous irradiation experiments (see Experimental Section). In the reaction of ^{1}perylene with **1**, the anion radical is so stable that there is no chance that the cation radical of perylene could react with the $NCPhCF_2$ radical within the solvent cage. Since, in addition, the cation radical of perylene is quite stable in the reaction medium, the quantum yield could be determined by means of laser flash experiments (see Experimental Section). Thus, in this case, but not in the others, $\Phi = \Phi_{D^{\bullet+}}$.

Table 2 also lists the rate constants of the photoinduced electron transfer derived from the fluorescence quenching experiments and/or the quantum yield measurements.

(12) (a) k_c, cleavage rate constant; k_S, electrochemical electron-transfer standard rate constant; D_d, diffusion coefficient. (b) Andrieux, C. P.; Tallec, A.; Tardivel, R.; Savéant, J.-M.; Tardy, C. *J. Am. Chem. Soc.* **1996**, *118*, 9788.

(13) Uncorrected for double-layer effects.

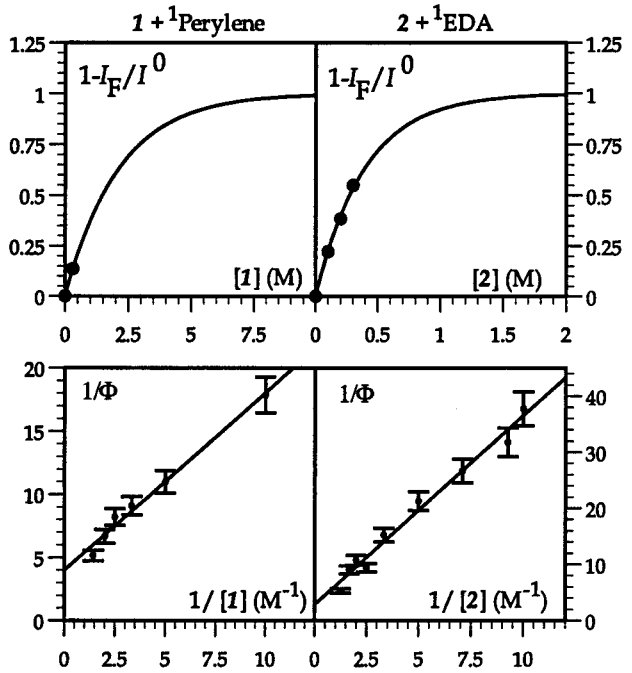

Figure 4. Fluorescence quenching (top) and quantum yields (bottom) in the reactions of **1** with ^{1}perylene and **2** with ^{1}EDA.

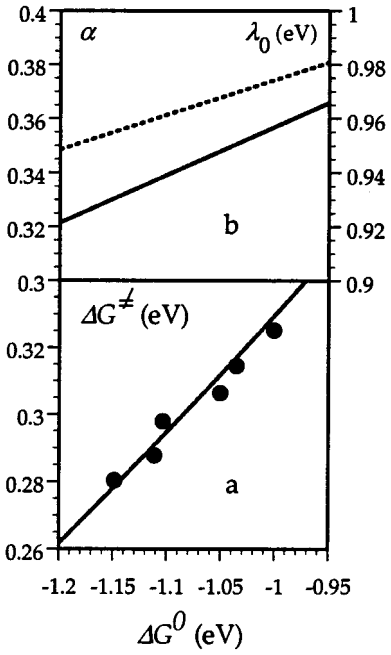

Figure 5. Electrochemical reductive cleavage of **4**. (a) Fitting of the experimental data by the theoretical $\Delta G^{\ddagger} - \Delta G^0$ relationship. Variation of the transfer coefficient (solid line) and of the solvent reorganization energy (dashed line) with ΔG^0.

Discussion

Thermal Reactions. The electrochemical reductive cleavages of **1** and **2** fall in the stepwise category. The anion radical of **1** is a rather stable species ($k_c = 38\ s^{-1}$) with a standard potential $E^0_{RX/RX^{\bullet -}} = -1.785$ V vs SCE.[10] With **2**, $9 \le \log k_c\ (s^{-1}) \le 9.5$ and $-1.9 \le E^0_{RX/RX^{\bullet -}}$ (V vs SCE) ≤ -1.85.

To treat properly the results obtained with **4** (Figure 1) in the framework of the dissociative electron-transfer theory,[3a] we need to take into account the possibility that a small but significant attractive interaction between the two fragments (charge-dipole and induced-dipole interaction between the chloride ion and the 4-cyanobenzyl radical) may persist in the solvent, as already found with 4-nitrobenzyl chloride[14] and carbon tetrachloride.[9b] The presence of the electron-withdrawing group in the para position indeed favors such an interaction. It is also important to take into account simultaneously the fact that the size of the volume to be solvated upon electron transfer is a function of the reaction coordinate.[15] Figure 5a shows the best fitting of the experimental points by the theoretical $\Delta G^{\ddagger} - \Delta G^0$ relationship ($\Delta G^{\ddagger}$, activation free energy; ΔG^0, standard free energy of reaction) corresponding to an interaction between the caged fragments of 58 meV and to a solvent reorganization energy which varies with the standard free energy of reaction as depicted in Figure 5b. The $\Delta G^{\ddagger} - \Delta G^0$ relationship is approximately quadratic, implying, as shown in Figure 5b, that the transfer coefficient (symmetry factor), α, varies linearly with ΔG^0. The fitting of the experimental data in Figures 2 and 5 with the theoretical curve was performed as follows.

As discussed elsewhere,[8b,9b,15] the energy profiles of the reactant and product systems obey eqs 5 and 6, respectively,

$$G_R = D_R Y^2 + \lambda_0(Y) X^2 \qquad (5)$$

$$G_P = \Delta G^0 - D_P + D_R\left(1 - \sqrt{\frac{D_P}{D_R}} - Y\right)^2 + \lambda_0(Y)(1 - X)^2 \qquad (6)$$

where ΔG^0 is the standard free energy of the reaction, D_R is the dissociation energy of the cleaving bond in the reactant, D_P is the energy of the interaction between the caged fragments, and Y is a coordinate representing the stretching of the cleaving bond. It is defined by eq 7, with $\beta = \nu(2\pi^2\mu/D_R)^{1/2}$, y is the

$$Y = 1 - \exp[-\beta(y - y_{RX})] \qquad (7)$$

bond length, y_{RX} is the equilibrium value of y in the reactant system, ν is the frequency of the cleaving bond, and μ is the reduced mass. X is a fictitious charge borne by the molecule, between 0 and 1, serving as an index for solvent reorganization. The solvent reorganization energy, λ_0, is a linear function of Y, defined by eq 8, in line with the assumption that the free energy profiles of the product system both in the gas phase and in the solvent may be represented approximately by Morse curves having the same repulsive term as the reactant Morse curve. In

$$\lambda_0(Y) = (1 - Y)\lambda_0^R + Y\lambda_0^P = \lambda_0^R + (\lambda_0^P - \lambda_0^R)Y \qquad (8)$$

eq 8, λ_0^R and λ_0^P, the reorganization energies for the reactant and product states, respectively, may be obtained from $\lambda_0^{R,P}$ (eV) $= 3/a_{R,P}$ (Å), where $a_R = 4.03$ Å[16] and $a_P = 1.81$ Å are the radii of the spheres equivalent to the 4-cyanobenzyl radical and Cl^-, respectively.

The activation free energy, $\Delta G^{\ddagger}$, is obtained by minimization of the two expressions in eqs 5 and 6, subject to the condition $G_R = G_P$, taking into account the variation of λ_0 with Y as depicted by eq 8. It follows that the following equations may be used to obtain the theoretical relationship between $\Delta G^{\ddagger}$ and ΔG^0:

(14) Costentin, C.; Hapiot, P.; Médebielle, M.; Savéant, J.-M. *J. Am. Chem. Soc.* **2000**, *122*, 5623.

(15) Andrieux, C. P.; Savéant, J.-M.; Tardy, C. *J. Am. Chem. Soc.* **1997**, *119*, 11546.

(16) (a) From $a = (3M/4N_A\rho)^{1/3}$ (M, molar mass; N_A, Avogadro's number; ρ, density).[16b] (b) Kojima, H.; Bard, A. J. *J. Am. Chem. Soc.* **1975**, *97*, 6317.

$$Y^{\ddagger} = \left(1 - \sqrt{\frac{D_P}{D_R}}\right)X^{\ddagger} - \frac{\lambda_0^P - \lambda_0^R}{2D_R}X^{\ddagger}(1 - X^{\ddagger}) \qquad (9)$$

$$\Delta G^0 = D_P + D_R\left(1 - \sqrt{\frac{D_P}{D_R}}\right)\left[2Y^{\ddagger} - \left(1 - \sqrt{\frac{D_P}{D_R}}\right)\right] + [\lambda_o^R + (\lambda_0^P - \lambda_0^R)Y^{\ddagger}](2X^{\ddagger} - 1) \qquad (10)$$

$$\Delta G^{\ddagger} = D_R Y^{\ddagger 2} + [\lambda_0^R + (\lambda_0^P - \lambda_0^R)Y^{\ddagger}]X^{\ddagger 2} \qquad (11)$$

A series of $\Delta G^{\ddagger} - \Delta G^0$ relationships is thus calculated for successive values of D_P until a good fit of the experimental data is reached, as shown in Figure 5a. D_R is taken as equal to 2.82 eV.[17a] The experimental values of ΔG^0 are derived from the peak potentials, E_p, according to eq 12, where

$$\Delta G^0 = E_p - E^0_{RX/R^{\bullet}+X^-}$$

$$\text{with } E^0_{RX/R^{\bullet}+X^-} = -D_R + E^0_{X^{\bullet}/X^-} + T(S_{R^{\bullet}} + S_{X^{\bullet}} - S_{RX}) \qquad (12)$$

$E^0_{RX/R^{\bullet}+X^-} = -0.71$ V vs SCE.[17b,c] The experimental values of $\Delta G^{\ddagger}$ are derived from eq 13, where $Z^{el} = (RT/2\pi M)^{1/2} = 5 \times 10^3$ cm s^{-1} (M is molar mass) is the electrochemical collision frequency, υ is the scan rate, and D (10^{-5} cm^2 s^{-1}) is the diffusion coefficient.

$$\Delta G^{\ddagger} = \frac{RT}{F}\left[\ln\left(Z^{el}\sqrt{\frac{RT}{\alpha F \upsilon D}}\right) - 0.78\right] \qquad (13)$$

The symmetry factor (transfer coefficient), α, is then given by eq 14.

$$\alpha = \frac{\partial \Delta G^{\ddagger}}{\partial \Delta G^0} = X^{\ddagger} \qquad (14)$$

We see (Figure 5b) that the variation of α with ΔG^0 is close to linear, implying that the $\Delta G^{\ddagger} - \Delta G^0$ relationship is close to quadratic. The variation of α with ΔG^0 is due essentially to the quadratic character of eqs 5 and 6, but also to the variation of the solvent reorganization energy with the reaction coordinate, as depicted by eq 9 (see the ensuing variation of λ_0 with ΔG^0 in Figure 5b).

The theoretical $E_p - \log \upsilon$ plot in Figure 1b was then derived from the equations relating E_p to ΔG^0 (eq 12) and υ to $\Delta G^{\ddagger}$ (eq 13), respectively.

The magnitude of the interaction between the caged fragments, 58 meV, falls in line with what has been previously found for 4-nitrobenzyl chloride, 105 meV,[14] and CCl_4, 62 meV.[9b]

The characteristics thus found will be used in the foregoing discussion of the photoinduced reductive cleavage of **4**.

Photoinduced Reactions. In the competition between the two pathways, an increase of the thermodynamic driving force favors the stepwise pathway over the concerted pathway.[3a] As recalled earlier, the electrochemical reductive cleavage of **1** and **2** follows a stepwise mechanism. Since the driving force in the photoinduced reactions is larger than that in the electrochemical reactions, the stepwise mechanism is a fortiori followed in the reaction of **1** and **2** with ^{1}perylene and ^{1}EDA, respectively. Owing to the fast follow-up separation of the two products, back electron transfer, and cleavage of the anion radical, the rate-determining step is the forward electron transfer between the ^{1}D and RX. The standard free energies of reaction, ΔG^0, for the two systems may be estimated as depicted in Table 3. The possible interaction between perylene$^{\bullet+}$ and **1**$^{\bullet-}$ has been neglected, in line with previous estimates of interaction energies in similar contact or solvent-separated ion pairs as a function of the solvent dielectric constant.[18] In the case of **2**, the interaction is even smaller since the "anion radical" of **2** is actually a neutral molecule. The reorganization energy, λ, mostly concerns solvent reorganization (λ_0), although, in view of the fast cleavage of **2**$^{\bullet}$, it is likely that a significant contribution to the reorganization energy may come from the lengthening of the cleaving bond upon electron transfer.[3,19] In the estimation of λ_0, the self-exchange solvent reorganization energies for ^{1}perylene and ^{1}EDA were taken as equal to those corresponding to the formation of the anion radicals of perylene and anthracene, respectively.[16b] For the reduction of **1** and **2**, we took the values for the formation of the anion radicals of *m*-nitrobenzonitrile and nitrobenzene, respectively.[16b] The rate constant thus estimated by application of the Marcus−Hush model[20] (Table 3) is consistent with the experimental value (Table 2) in the case of ^{1}perylene + **1**, while the predicted value is too large by ca. 1 order of magnitude in the case of ^{1}EDA and **2**. The latter discrepancy is likely due to the neglect of the internal reorganization, as just discussed.

The electrochemical reductive cleavage of **4** follows a concerted mechanism within the range of driving forces that we have explored. Since the driving force offered by the photoinduced reaction is larger, the possibility that the mechanism could switch to the stepwise case should be envisaged. The thermodynamics is largely in favor of the concerted pathway, the electron transfer in the stepwise process being an uphill reaction (Table 3). However, the reorganization energy is certainly larger in the first case than in the second since the breaking of the bond is part of the nuclear reorganization attending electron transfer.

If, in the evaluation of the stepwise pathway, internal reorganization is neglected compared to solvent reorganization, an activation free energy of 0.262 eV and thus a rather low rate constant, 6×10^6 M^{-1} s^{-1}, are predicted (Table 3). The actual rate constant is most probably lower because of the interference of internal reorganization for the same reasons as previously discussed for **2**. A rate constant of 6×10^5 M^{-1} s^{-1} is thus more likely.

In the estimation of the rate constant for the concerted pathway, we have to take into account the attractive interaction between the fragments within the solvent cage as in the treatment of the electrochemical reaction. We thus used the same equations (eqs 9−11), taking for λ_0^R the average between the λ_0 values of anthracene and *m*-nitrobenzonitrile and for λ_0^P the average between the λ_0 values of anthracene and Cl^- (1.66 eV). Taking for the energy of interaction between the caged fragments D_P = 58 meV, we thus obtain $\Delta G^{\ddagger} = 0.184$ eV, and thus $k_{et} = 1.5 \times 10^8$ M^{-1} s^{-1}. The concerted mechanism is thus unambiguously followed, not only during the electrochemical reaction but also in the photoinduced process. The rate constant thus predicted is in fact smaller than the experimental value by almost 1 order of magnitude. This may be explained by the fact that the presence of the positively charged EDA cation radical and 4-CNPh$^{\bullet}$ is likely to enhance its interaction with Cl^-. Increasing the value of D_P up to 100 meV suffices to predict a rate constant of 10^9 M^{-1} s^{-1}.

What about the reductive cleavage of **3** by ^{1}EDA? The question of the stepwise/concerted dichotomy is of particular interest in this case since the reaction was originally claimed to be of the stepwise type, in contrast with the electrochemical reaction, based on the observation of a quantum yield less than

Table 3. Thermodynamic and Kinetic Characteristics of the Photoinduced Reductive Cleavage and of the Back Electron Transfer[a]

			photoinduced reductive cleavage $^1D + RX \rightarrow D^{\bullet+} + RX^{\bullet-}$ or $^1D + RX \rightarrow D^{\bullet+} + R^{\bullet} + X^-$				back electron transfer $(D^{\bullet+},RX^{\bullet-}) \rightarrow D + RX$ or $(D^{\bullet+},R^{\bullet},X^-) \rightarrow D + RX$			
system	mechanism	$E^0_{RX/RX^{\bullet-}}$ or $E^0_{RX/R^{\bullet}+X^-}$	$\Delta G^{0\,c}$	λ^d	$\Delta G^{\ddagger\,g}$	$k_{et}{}^h$	$\Delta G^{0\,k}$	λ^d	region	k_{-act} or H^l
^{1}perylene + **1**	stepwise	−1.78	−0.03	0.6	0.133	9×10^8	−2.81	0.60	inverted	1.5×10^9
^{1}EDA + **2**	stepwise	−1.90 to −1.85	−0.101 to −0.151	0.70	0.128 to 0.108	1×10^9 to 1.5×10^9	−2.90 to −2.85	0.70	inverted	0.8×10^9 to[m] 1×10^{10}
^{1}EDA + **3**	stepwise	−1.80	−0.21	0.70	0.086	4×10^9	−2.80	0.70	inverted	$\cong 3 \times 10^9$ [n]
	concerted	−0.2[b]	−1.81	2.75[e]	0.080	5×10^9	−1.20	2.75	normal	0.013[f]
^{1}EDA + **4**	stepwise	−2.2	0.19	0.60	0.262	6×10^6 [i]	−3.2	0.60		
	concerted	−0.71[b]	−1.30	*f*	0.184	1.5×10^8 [j]	−1.71	see text	normal	0.017[f]

[a] Energies in eV, bimolecular rate constant in $M^{-1}\,s^{-1}$, monomolecular rate constants in s^{-1}. [b] $E^0_{RX/R^{\bullet+}X^-} = -D_R + E^0_{X^{\bullet}/X^-} + T(S_{R^{\bullet}} + S_{X^{\bullet}} - S_{RX})$ with $E^0_{Cl^{\bullet}/Cl^-} = 1.81$ V vs SCE[9b] and $E^0_{PhSCH_3{}^{\bullet+}/PhSCH_3} = 1.56$ V vs SCE,[4c] $D_R = 2.07$ and 2.82 eV for **3**[4c] and **4**,[17a] respectively. $T(S_{R^{\bullet}} + S_{X^{\bullet}} - S_{RX}) = 0.3$ eV.[17b] [c] $\Delta G^0 = E^0_{D^{\bullet+}/{}^1D} - E^0_{RX/RX^{\bullet-}}$ or $\Delta G^0 = E^0_{D^{\bullet+}/{}^1D} - E^0_{RX/R^{\bullet}+X^-}$ with $E^0_{D^{\bullet+}/{}^1D} = -E_{D\rightarrow{}^1D} + E^0_{D^{\bullet+}/D} = -3.01 + 1.00 = -2.01$ V vs SCE for EDA and $-2.84 + 1.03 = -1.81$ V vs SCE for perylene, respectively. [d] $\lambda = \lambda_0 + \lambda_i + (D$ in the case of a dissociative process), with $\lambda_0 = (\lambda_0^{{}^1D} + \lambda_0^{RX})/2$. [e] $D = 2.05$ eV, $\lambda_0 = 0.7$ eV. [f] See text. [g] $\Delta G^{\ddagger} = (\lambda/4)(1 + \Delta G^0/\lambda)^2$, unless otherwise stated. [h] $1/k_{et} = 1/k_{act} + 1/k_d$ with $k_{act} = Z\exp(F\Delta G^{\ddagger}/RT)$. Z, the bimolecular collision frequency, is equal to 2×10^{11} $M^{-1}\,s^{-1}$ on average and k_d, the diffusion-limited rate constant, to 10^{10} $M^{-1}\,s^{-1}$ on average. [i] More likely 6×10^5 $M^{-1}\,s^{-1}$, as discussed in the text. [j] With $D_P = 58$ meV. With $D_P = 100$ meV, $k_{et} = 10^9$ $M^{-1}\,s^{-1}$. [k] $\Delta G^0 = E^0_{RX/RX^{\bullet-}} - E^0_{D^{\bullet+}/D}$ or $\Delta G^0 = E^0_{RX/R^{\bullet}+X^-} - E^0_{D^{\bullet+}/D}$. [l] $k_{sp} = 5 \times 10^8$ s^{-1}. [m] $8 \times 10^8 \le k_c \le 5 \times 10^9$ s^{-1}. [n] $k_c = 10^{10}$ s^{-1} (estimated).

unity and on the intuition that concerted reactions are endowed with a unity quantum yield.[7d] We now know that the quantum yield of concerted electron-transfer/bond-breaking reactions is not necessarily equal to unity.[8,9c] However, it should be envisaged that the mechanism could switch from concerted to the stepwise when passing from the electrochemical to the photochemical conditions as a result of the attending increase of the driving force. We have followed the same strategy as for ^{1}EDA + **4** to compare the two pathways, with the difference that the attractive interaction between the caged fragments may now be neglected since both fragments are neutral. It is interesting to note that the probabilities of the two pathways are very similar, with only a slight disadvantage for the stepwise reaction (Table 3). It should be again emphasized that the occurrence of the stepwise pathway under these conditions, as opposed to the electrochemical case, is not indicated by the fact that the quantum yield is less than unity and results from the fact that the driving force is larger in the first case than in the second. In fact, the probability for the stepwise pathway to be followed is somewhat less than that indicated by the above discussion because some internal reorganization should be taken into account, just as in the case of **2**. Consideration of this effect would diminish the probability of the stepwise pathway by a factor of ca. 10, which would nevertheless leave the system in a borderline situation.

We may now examine whether the values of the quantum yields (Table 2) are consistent with reasonable values of the rate constants of back electron transfer, taking account of product separation and cleavage of the anion radical. However, before discussing this point, we must check whether the quantum yield does exclusively reflect the competition between these reactions or whether it is additionally affected by electron transfer from X^- (Cl^-, F^-, $PhSCH_3$) or from $R^{\bullet}$ to $D^{\bullet+}$, followed by the coupling between $X^{\bullet}$ ($Cl^{\bullet}$, $F^{\bullet}$, $PhSCH_3{}^{\bullet+}$) and $R^{\bullet}$ or between R^+ and X^-, regenerating RX, and thus diminishing the quantum yield, in both cases. A careful analysis of the question[7d] has shown that, in the case of ^{1}EDA + **3**, these additional reactions can be neglected, in line with the fact that the standard potentials for the oxidation of $NCPhCH_2{}^{\bullet}$ and $PhSCH_3$ are more positive (1.08 [20] and 1.56 [4c] V vs SCE, respectively) than the EDA standard potential (1.00 V vs SCE [9c]). The same is a fortiori true with the reaction of ^{1}EDA with **4**, since $E^0_{Cl^{\bullet}/Cl^-} = 1.81$ V vs SCE.[17c] The oxidations of $NCPhCF_2{}^{\bullet}$ and of F^- are thermodynamically more difficult than the oxidations of $NCPhCH_2{}^{\bullet}$ and of Cl^-, respectively. The above side reactions may thus be neglected in this case too. The same conclusion applies to the case of ^{1}EDA + **2**, since the standard potential for the oxidation of the methyl radical is 1.80 V vs SCE.[21]

The possibility of another side reaction should also be examined, namely the radical−radical coupling of $D^{\bullet+}$ with $R^{\bullet}$, leading to $^+$DR, which could then combine with X^-, finally yielding an XDR compound (Scheme 3). Insofar as these reactions are so rapid as to occur within the solvent cage, they consume X^- and therefore diminish the value of the quantum yield when this is measured through the production of this compound. This possibility was ruled out in the case of the ^{1}EDA + **3** after inspection of the reaction products.[7d] The occurrence of the same reaction was also ruled out in the reaction of ^{1}EDA + CCl_4.[9c] In the case of **4**, the cation $^+$DR is less electrophilic than with CCl_4. It is thus less likely to react with Cl^-, which rules out the occurrence of the reaction. With **2**, the electrophilicity of $^+$DR is equal to or less than that with **3**, making the reaction negligible in this case, too. Finally, with

(17) (a) Pratt, D. E.; Wright, J. S.; Ingold, K. U. *J. Am. Chem. Soc.* **1999**, *121*, 4877. (b) $T(S_{R^{\bullet}} + S_{X^{\bullet}} - S_{RX}) = 0.3$ eV,[14,15] and $E^0_{Cl^{\bullet}/Cl^-} = 1.81$ V vs SCE.[9b]

(18) (a) Gould, I. R.; Ege, D.; Moser, J. E.; Farid, S. *J. Am. Chem. Soc.* **1990**, *112*, 42907. (b) Gould, I. R.; Young, R. H.; Moody, R. E.; Farid, S. *J. Am. Chem. Soc.* **1991**, *113*, 2068. (c) Gould, I. R.; Farid, S. *Acc. Chem. Res.* **1996**, *29*, 522. (d) Arnold, B. R.; Farid, S.; Goodman, J. L.; Gould, I. R. *J. Am. Chem. Soc.* **1996**, *118*, 5482.

(19) (a) Savéant, J.-M. *J. Phys. Chem.* **1994**, *98*, 3716. (b) Savéant, J.-M. *Tetrahedron* **1994**, *50*, 10117.

(20) Clark, K. B.; Wayner, D. D. M. *J. Am. Chem. Soc.* **1991**, *113*, 9363.

(21) from $E^0_{t\text{-}Bu^+/t\text{-}Bu^{\bullet}} = 0.09$ V vs SCE[21b] and the standard free enthalpy of the reaction $CH_3{}^{\bullet} + t\text{-}Bu^+ \rightarrow CH_3{}^+ + t\text{-}Bu^{\bullet}$ derived from a quantum chemical ab initio calculation involving geometry optimization and energy calculation at the UHF-MP2 level, followed by calculation of the standard free enthalpy of solvation according to the IPCM method (using the Gaussian 98 package[21c]). (b)Wayner, D. D. M.; McPhee, D. J.; Griller, D. *J. Am. Chem. Soc.* **1988**, *110*, 132. (c) Frisch, M. J.; Trucks, G. W.; Schlegel, H. B.; Scuseria, M. A.; Gill, P. M. W.; Johnson, B. G.; Robb, M. A.; Cheeseman, J. R.; Keith, T.; Petersson, G. A.; Montgomery, J. A.; Stratmann, R. E.; Burant, J. C.; Dapprich, S.; Millam, J. M.; Daniels, A. D.; Kudin, K. N.; Strain, M. C.; Farkas, O.; Tomasi, J.; Barone, V.; Cossi, M.; Cammi, R.; Mennuci, B.; Pomelli, C.; Adamo, C.; Clifford, S.; Ochterski, G.; Cui, Q.; Morokuma, K.; Malick, D. K.; Rabuck, A. D.; Raghavachari, K.; Al-Laham, M. A.; Zakrzewski, V. G.; Ortiz, J. V.; Foresman, J. B.; Cioslowski, J.; Stefanov, B. B.; Liu, G.; Liashenko, A.; Piskorz, P.; Komaromi, I.; Nanayakkara, A.; Challacombe, M.; Peng, C. Y.; Ayala, P. Y.; Chen, W.; Wong, M. W.; Andres, J. L.; Replogle, A. S.; Gomperts, R.; Martin, R. L.; Fox, D. J.; Binkley, J. S.; Defrees, D. J.; Baker, J.; Stewart, J. P.; Head-Gordon, M.; Gonzalez, C.; Pople, J. A. *Gaussian 98*, Revision A.1; Gaussian, Inc.: Pittsburgh, PA, 1998.

Scheme 3

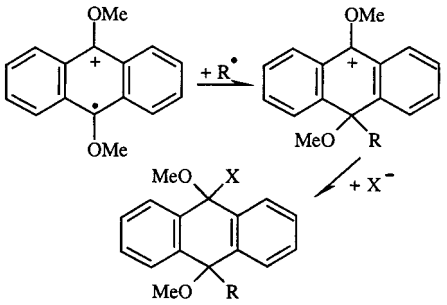

1, the cleavage is so slow ($k_c = 38\ s^{-1}$) that the formation of R• does not occur in the vicinity of EDA•+, making the first step in Scheme 3 inefficient.

Thus, for all investigated systems, the quantum yield is a reflection of the competition between back electron transfer on one hand and product separation and anion radical cleavage on the other. As summarized in Table 3, in all stepwise processes, the initial electron transfer falls in the inverted region. The quantum yield is then given by eq 2 as a function of the rate constants for the escape from the solvent cage, k_{sp}, for cleavage, k_c, and for back electron transfer, k_{-act}.

In the case of **1**, the cleavage is so slow ($k_c = 38\ s^{-1}$) that it has no effect on the magnitude of the quantum yield. In this case, as in the others, there is some uncertainty in the exact value of k_{sp}. On one hand, if electrostatic interaction is negligible in polar solvents such as acetonitrile[18d] (and DMF), k_{sp} (s^{-1}) should be equal to the value of k_d (in $M^{-1}\ s^{-1}$) in DMF, i.e., $10^{10}\ s^{-1}$. Application of eq 2 would then lead to $k_{-act} = 3.3 \times 10^{10}\ s^{-1}$, which is too large a value by comparison with similar photoinduced reactions.[18a−c] A value of $5 \times 10^8\ s^{-1}$ for k_{sp}, leading to $k_{-act} = 1.5 \times 10^9\ s^{-1}$, seems more reasonable. If we take the same value of k_{sp} for the ^{1}EDA + **2** and ^{1}EDA + **3** systems, values of k_{-act} (Table 3) of the same order as for similar systems are again found. It is interesting to note that, for the stepwise processes, the fact that the quantum yield increases in the order **1** < **2** < **3** is essentially a consequence of the cleavage becoming faster and faster in the series.

In the two concerted cases, back electron transfer within the caged fragment cluster stands in the normal region. The quantum yield then obeys eq 1. The ratio between the rate constants for cage coupling and for fragment separation may be derived from the ratio of the two quantum yields at a quencher concentration equal to 1.3 M, $\Phi_{D^{\bullet+}} = 0.16$ and $\Phi = 0.4$, according to eq 15. Thus, $k_{sp} = 5 \times 10^8\ s^{-1}$ and $k_{cc} = 7.5 \times 10^8\ s^{-1}$. After

$$\frac{\Phi_{D^{\bullet+}}}{\Phi} = \frac{k_{sp}}{k_{sp} + k_{cc}} = 0.4 \qquad (15)$$

estimation of the back electron transfer rate constant, k_{-act}, eq 1 may be used to estimate the probability p and, from it, the predicted magnitude of the electronic coupling matrix element, H. The ratio of the forward to the backward electron transfer rate constants in the ground state is strongly in favor of the latter reaction,

$$\frac{k_{act}}{k_{-act}} = \exp\left(-\frac{F(\Delta G^0_+ - D_P)}{RT}\right) = 2.02 \times 10^{-28}\ M^{-1}$$

$$\text{and} \quad k_{act} = Z \exp\left(-\frac{F\Delta G^{\ddagger}_+}{RT}\right)$$

$\Delta G^{\ddagger}_+$ may then be obtained by the same procedure that we have used for estimating the rate constant of the reaction of ^{1}EDA + **4**, taking into account, in the same manner, the attractive interaction between the fragments in the product cluster and the variation of the solvent reorganization energy along the reaction coordinate. We thus find $\Delta G^{\ddagger}_+ = 1.729$ eV, $k_{act} = 3.6 \times 10^{-19}\ M^{-1}\ s^{-1}$, and $k_{-act} = 1.8 \times 10^9\ s^{-1}$ ($\lambda_0 = 0.9$ eV). Thus, from eq 1, $p = 0.21$. From eq 4,

$$H = \left[-\frac{h\nu(RT)^{1/2}(D + \lambda_0)^{1/2}}{\pi^{3/2}} \ln(1 - p)\right]^{1/2}$$

Taking $\nu = 6.2 \times 10^{12}\ s^{-1}$,[22] and $D + \lambda_0 = (D_R^{1/2} - D_P^{1/2})^2 + \lambda_0 = 2.76$ eV, we find that $H = 0.017$ eV, indicating that the ground-state electron-transfer reaction is moderately nonadiabatic.

Coming to the concerted pathway in the reaction of ^{1}EDA with **3**, a similar treatment ($k_{sp} = 5 \times 10^8\ s^{-1}$, $k_{cc} = 1.5 \times 10^9\ s^{-1}$, as in the preceding case; $p = 0.08$, $\nu = 1.1 \times 10^{13}\ s^{-1}$,[22] $D + \lambda_0 = 2.71$ eV) leads to $H = 0.013$ eV, a quite reasonable value in the present case, too.

Conclusions

Of the four compounds investigated, **1** and **2** undergo a stepwise electrochemical reductive cleavage going through the intermediacy of their anion radicals. The same mechanism is a fortiori followed in their reaction with ^{1}perylene and ^{1}EDA, respectively, since photoinduction offers more driving force than electrochemical reduction and since an increase of the driving force pushes the mechanism from concerted to stepwise. The predictions for the rate constant of the initial electron-transfer reaction based on thermodynamic and kinetic characteristics of their electrochemical reduction are consistent with the values found from fluorescence quenching. Being driven by a very negative standard free energy, back electron transfer in both photoinduced reactions lies in the inverted region of the activation−driving force correlation, giving rise to back electron transfers in the nanosecond regime as estimated from the value of the complete quenching quantum yield. The larger value of the quantum yield found with **2** than with **1** results from the cleavage being much faster with **2** than with **1**, becoming then able to compete with back electron transfer.

In contrast, the electrochemical reductive cleavage of **4** follows a concerted mechanism. The same mechanism is also followed in the photoinduced reaction despite the increased driving force. The kinetics of the electrochemical reduction fits with the dissociative electron-transfer model, provided a small attractive interaction between the caged fragments is allowed for. The rate constants of fluorescence quenching are consistent with predictions based on the thermodynamic and kinetic characteristics derived from cyclic voltammetry. Analysis of the quantum yield taking into account back electron transfer, fragment separation, and partitioning of the system at the intersection of the product and ground-state potential energy surfaces allows an estimation of the electronic matrix element coupling the fragmented product state and the ground reactant state, thus leading to a quite reasonable value.

The case of the reaction of ^{1}EDA with **3** is of particular interest since the reaction was originally thought to be of the stepwise type, in contrast with the electrochemical reaction shown to be of the concerted type, based on the observation of

(22) (a) From $\nu = (\nu_c/2)[1 - \{\Delta G^0_+/[(D_R^{1/2} - D_P^{1/2})^2 + \lambda_0]\}^2]$,[8a,9c] where ν_c, the asymmetric stretching frequency of the cleaving bond, is equal to 690 and 946 cm^{-1} for **4** and **3**, respectively.[22b] (b) Pachler, K. G. R.; Matlok, F.; Gremlich, H. V. *Merck FT−IR Atlas*; VCH: Weinheim, 1988.

a quantum yield less than unity and on the intuition that concerted reactions are endowed with a unity quantum yield. Although we now know that the latter assertion is not correct, there is still the possibility of a passage from a concerted mechanism to a stepwise mechanism, owing to the increase of driving force taking place when going from the electrochemical to the photochemical conditions. Such a trend indeed results from the analysis of the experimental results. The change in the mechanism is, however, not complete since we find that in the photoinduced reaction, there is a balanced competition between the two pathways. In the same families of compounds, the unsubstituted benzylmethylphenyl sulfonium cations shows such a borderline behavior during the electrochemical reaction. In the photoinduced reaction, it is the 4-cyano derivative which behaves in a borderline manner, in accord with the fact that it gives rise more readily to a concerted mechanism that the unsubstituted compound.

Experimental Section

Chemicals. *N*,*N*′-Dimethylformamide (Fluka, >99.5%, stored on molecular sieves under an argon atmosphere), perylene (Acros, 99+%), and **1** (Aldrich, 99%) were used as received. 2-Ethyl-9,10-dimethoxyanthracene (Aldrich, 97%) was recrystallized twice from Et_2O before use.

2 (Phenyldimethyl Sulfonium Trifluorosulfonate). Phenylmethyl sulfide (0.05 mol, Aldrich) was dissolved in methylene chloride (40 mL) and cooled in an ice bath before dropwise addition of methyltrifluorosulfonate (0.05 mol, Fluka). The mixture was refluxed for 15 h, cooled, and poured into 150 mL of diethyl ether. The product then crystallized and was finally collected by suction filtration and air-dried. Recrystallization from isopropyl alcohol gave a 95% yield. ^{1}H NMR (acetone-d_6): δ 3.26 (s, 6H). Anal. Calcd for $C_9H_{11}S_2F_3O_3$: C, 37.7; H, 3.8. Found: C, 37.4; H, 3.9.

4 (4-Cyanobenzyl Chloride). 4-Cyanobenzyl bromide (Aldrich, 99%) was dissolved in an acetone/dichloromethane (50/50) mixture in the presence of a 10-fold excess of tetraethylammonium chloride (Acros, 99%) and then refluxed for 1 h. After evaporation and addition of ether, the remaining salt precipitated, and the organic phase was filtered and evaporated. **4** was recrystallized from a pentane/dichloromethane (60/40) mixture, leading to an 84% yield of pure compound. The structure was checked by ^{1}H NMR and elemental analysis.

Cyclic Voltammetry. The working electrode was a 3- or a 1-mm-diameter glassy carbon electrode disk (Tokai), carefully polished and ultrasonically rinsed in absolute ethanol before use. The counter electrode was a platinum wire and the reference electrode an aqueous SCE electrode. The potentiostat, equipped with positive feedback compensation and current measurer, was the same as previously described.[23] All experiments have been carried out at 20 °C, the double-wall jacket cell being thermostated by circulation of water.

Photochemical Experiments. (i) Laser Flash Photolysis. The samples were irradiated with an intense nanosecond excimer laser (XeCl, $\lambda = 308$ nm, $E = 110$ mJ). The optical detection of transient species was performed perpendicularly to the laser beam with an optical multichannel analyzer (Princeton Instruments), allowing the recording of absorption spectra a few tens of nanoseconds after the pulse. Acquisition of each spectrum was made over a time window of 100 ns. Quantum yields for radical cation formation, $\Phi_{D^{\bullet+}}$, were estimated using the benzophenone triplet as an actinometer. The ΔOD values of the benzophenone triplet (monitored at 520 nm) and of the radical cations (monitored at 550 nm for $EDA^{\bullet+}$ and 552 nm for $perylene^{\bullet+}$) were measured immediately after excitation as a function of laser intensity, which was modulated by appropriate filters. Both solutions of benzophenone and aromatic donors were prepared so that they were optically matched at 308 nm. The plots of ΔOD vs laser dose were linear at low laser power. The quantum yields were thus obtained using the slopes extrapolated at zero intensity ($S^{\bullet+}$ for the radical cation, S^{benz} for benzophenone) and by using the molar extinction coefficient of the two species ($\epsilon^{\bullet+}$ for the radical cation and $\epsilon^{benz} = 7200$ M^{-1} cm^{-1} for benzophenone) according to

$$\Phi_{D^{\bullet+}} = \Phi^{benz}\epsilon^{benz}S^{\bullet+}/S^{benz}\epsilon^{\bullet+}$$

where the quantum yield for benzophenone formation, Φ^{benz}, is equal to 1.

(ii) Fluorescence Quenching Experiments. Steady-state fluorescence quenching experiments were carried out with a Perkin-Elmer LS5 fluorimeter. Perylene fluorescence extends from 450 to 600 nm, and between 425 and 575 nm with 2-ethyl-9,10-dimethoxyanthracene (EDA). Stern−Volmer plots were obtained by adding increasing amounts of substrate and measuring the decrease of the fluorescence emission band at 480 and 508 nm with perylene and at 445 nm with EDA. No new emission bands appear upon addition of quencher.

Quantum Yields of Chloride Formation (^{1}EDA + 4). Solutions containing 2−2.5 mM EDA and variable concentrations of the cleaving quencher were irradiated with filtered UV light (321 ± 10 nm from an interferometric filter, Andover Corp.) coming from a high-pressure short arc xenon lamp (150 W, Oriel). The solutions were carefully deaerated with argon bubbling prior to irradiation, and the yields of chloride anion were measured for illumination times varying between 360 and 600 s. The highest quantities of Cl^- produced during these experiments correspond to less than 5% of the initial quantity of sensitizer. The quantum yields were observed to be independent of time.

Chloride concentration was determined by ionic chromatography (Dionex DX100 equipped with a conductometric detector, a conductivity suppresser, ASRS-I 4 mm, and a Dionex IonPac AS14-SC ionic exchange column of 4 mm diameter). Samples were diluted in ultrapure water in a 1/50 ratio prior to injection for analysis. The peak area was proportional to chloride concentration, and the concentrations were obtained by comparison with a calibration curve (from tetraethylammonium chloride in the same solvent mixture), which was systematically repeated after each experiment. Although the chloride concentrations are small ($\leq$10 μM after the 1/50 dilution), accurate measurements could be performed thanks to the sensitivity of ion chromatography.

Determination of the quantum yield also requires knowing the concentration of photons absorbed during irradiation according to the equations below. This was achieved by measuring light intensity using an Aberchrome 540 (Aberchromics Ltd.) as a chemical actinometer:[24]

$$I = \frac{\Delta\mathrm{OD}\ V}{\Phi_0 \epsilon t} \qquad \text{and} \qquad \Phi_{Cl^-} = \frac{[Cl^-]V}{It}$$

where I is the intensity of the light (einstein s^{-1}), ΔOD is the increase in absorbance at 494 nm for A_{540}, V is the volume of

(23) Garreau, D.; Savéant, J.-M. *J. Electroanal. Chem.* **1972**, *35*, 309.

(24) (a) Hatchard, C. G.; Parker, C. A. *Proc. R. Soc. London A* **1956**, *235*, 518. (b) Heller, H. G.; Langan, J. R. *J. Chem. Soc., Perkin Trans. 2* **1981**, 341.

the solution irradiated (10 cm^3 in our case), t is the irradiation time, $\Phi_0 = 0.20$ is the quantum yield for the transformation of A_{540}, and $\epsilon = 8200\ M^{-1}\ cm^{-1}$ is the molar extinction coefficient of the photoproduct. The amount of photons was measured after each experiment, and care was taken that all incident light is absorbed. Each quantum yield was measured at least twice. The accuracy may be estimated as better than 13% (8−10% for the Cl^- concentration and 2−3% for the photon concentration).

Quantum Yields of Sulfide Formation (^{1}EDA + 2). Solutions containing the aromatic donor (10 mM in EDA) and the quencher were irradiated with filtered UV light (321 ± 10 nm from an interferometric filter, Andover Corp.) coming from a high-pressure short arc xenon lamp (150 W, Oriel). Solutions were carefully deaerated with argon bubbling prior to irradiation, and the yields of sulfide were measured for illumination times varying between 360 and 600 s. The highest quantities of $PhSCH_3$ produced during these experiments correspond to less than 0.5% of the initial quantity of sensitizer. The quantum yields were found to be time independent. The sulfide concentration was determined by high-performance liquid chromatography using a Gilson apparatus equipped with a Kromasil column (C18, 100 Å, 4.6 mm × 250 mm, Colochrom), UV detection at 254 nm, eluent 70/30 CH_3CN/H_2O (flow rate, 1 mL/min). Samples were diluted in ultrapure water in a 1/50 ratio prior to injection for analysis. The peak area was proportional to sulfide concentration, and the concentration was finally obtained by comparison to a calibration curve (from an authentic sample in the same solvent mixture) systematically after each experiment. The concentration of photons absorbed during irradiation was determined as in the preceding case. The accuracy of the quantum yields is estimated to be between 9 and 12%.

JA004234U